Cancer Immunology, Immunotherapy (2025) 74:211
https://doi.org/10.1007/s00262-025-04079-z

RESEARCH

NECTIN4 regulates the cell surface expression of CD155 in non-small cell lung cancer cells and induces tumor resistance to PD-1 inhibitors

Shun Mizusaki[1] · Yasuto Yoneshima[1] · Eiji Iwama[1] · Tadayuki Nakashima[1] · Ritsu Ibusuki[1] · Daisuke Shibahara[1] · Kohei Otsubo[1] · Kentaro Tanaka[1] · Isamu Okamoto[1]

Received: 26 November 2024 / Accepted: 3 May 2025

Abstract

The development of immune checkpoint inhibitors has changed treatment strategies for some patients with non-small cell lung cancer (NSCLC). However, resistance remains a major problem, requiring the elucidation of resistance mechanisms, which might aid the development of novel therapeutic strategies. The upregulation of CD155, a primary ligand of the immune checkpoint receptor TIGIT, has been implicated in a mechanism of resistance to PD-1/PD-L1 inhibitors, and it is therefore important to characterize the mechanisms underlying the regulation of CD155 expression in tumor cells. The aim of this study was to identify a Nectin that might regulate CD155 expression in NSCLC and affect anti-tumor immune activity. In this study, we demonstrated that NECTIN4 regulated the cell surface expression and stabilization of CD155 by interacting and co-localizing with CD155 on the cell surface. In a syngeneic mouse model, NECTIN4-overexpressing cells exhibited increased cell surface CD155 and resistance to anti-PD-1 antibodies. Of note, combination therapy with anti-PD-1 and anti-TIGIT antibodies significantly suppressed tumor growth. These findings provide new insights into the mechanisms of resistance to anti-PD-1 antibodies and suggest that NECTIN4 could serve as a valuable marker in therapeutic strategies targeting TIGIT.

Keywords Poliovirus receptor (PVR) · Nectin-like molecule-5 (Necl5) · T-Cell immunoreceptor with Ig and immunoreceptor tyrosine-based inhibitory domains (TIGIT) · Non small cell lung cancer (NSCLC)

Introduction

Immune checkpoint inhibitors, which target the inhibitory signaling in T cells mediated by the interaction of PD-1 with its ligand PD-L1, have shown unprecedented clinical activity for the treatment of non-small cell lung cancer (NSCLC) and have become a standard of care (1–4). However, the efficacy of immune checkpoint inhibitors is still insufficient because of challenges related to primary and acquired resistance (5). Several mechanisms of resistance to PD-1/PD-L1 inhibitors have been reported, including the suppression of T cells by immune checkpoint molecules other than those in the PD-1/PD-L1 axis (6–9). Among these molecules, T-cell immunoreceptor with Ig and immunoreceptor tyrosine-based inhibitory domains (TIGIT) is an immune checkpoint receptor that is regarded as a potential new therapeutic target (7, 10–12).

CD155, also known as Poliovirus receptor (PVR) or Nectin-like molecule-5 (Necl-5), is involved in tumor immunity as a ligand for the co-inhibitory molecules TIGIT and CD96, and the co-stimulatory molecule CD226 (13, 14), and is considered a major ligand of TIGIT because of its high affinity (11). CD155 is widely expressed in normal tissues and is often overexpressed in various types of cancer, which correlates with tumor progression and poor prognosis (14–18). The high expression of CD155 in tumor tissues was reported to be associated with the reduced therapeutic efficacy of anti-PD-1 antibody in patients with NSCLC (19). Therefore, understanding the regulatory mechanisms of CD155 in cancer cells may help to overcome resistance to PD-1/PD-L1 inhibitor therapy.

The Nectin family consists of four members, NECTIN1, NECTIN2, NECTIN3, and NECTIN4 (20, 21), which are adhesion molecules that not only form adherens junctions but also function as viral receptors (20, 21). It was reported

✉ Yasuto Yoneshima
yoneshima.yasuto.926@m.kyushu-u.ac.jp

[1] Department of Respiratory Medicine, Graduate School of Medical Sciences, Kyushu University, 3-1-1 Maidashi, Higashi-ku, Fukuoka 812-8582, Japan

Published online: 20 May 2025

that some Nectins were involved in the regulation of the cell surface expression of CD155 in a murine model. In mouse fibroblasts and liver cancer, NECTIN3 induces the internalization of CD155 through intercellular interactions, and NECTIN1 suppresses the NECTIN3-mediated internalization of CD155 by binding to NECTIN3, resulting in the stabilization of CD155 on the cell surface (22, 23). However, it remains unclear whether Nectin family members regulate CD155 expression and affect anti-tumor immunity in humans.

We investigated the potential role of Nectins in the regulation of CD155 expression in human NSCLC and the induction of tumor resistance to PD-1 inhibitors.

Materials and methods

Cell lines and cell culture

HEK293T (RRID: CVCL_0063), A549 (RRID: CVCL_0023), EBC1 (RRID: CVCL_2891), H1299 (RRID: CVCL_0060), H1437 (RRID: CVCL_1472), H2009 (RRID: RRID: CVCL_0125), 4T1 (RRID: CVCL_0125), CT26 (RRID: CVCL_7254), and LL/2 (RRID: CVCL_4358) cell lines were obtained from the American Type Culture Collection (Manassas, Virginia, USA), and H322 (RRID: CVCL_1556) was from the European Collection of Authenticated Cell Cultures (Salisbury, UK). All cells were confirmed to be mycoplasma-negative before use and were maintained under a humidified atmosphere of 5% CO_2 at 37℃ in RPMI 1640 medium (Gibco, Carlsbad, California, USA, #11,875,119), Dulbecco's modified Eagle's medium (Gibco, #11,320,082), or MEM medium with Earle's Salts and L-Gln (Nacalai Tesque, Kyoto, Japan, #21,442–25), each supplemented with 10% fetal bovine serum and 1% penicillin–streptomycin (Thermo Fisher Scientific, Waltham, MA, USA, #15,140,122).

Plasmid constructs and establishment of stable cell lines

Expression vectors for the target genes were created using the pQCXIP retroviral vector (RRID: Addgene_15714) (Takara Bio, Mountain View, CA, USA, #631,516), with the use of an In-Fusion HD Cloning Kit (Takara Bio, #639,648). The pQCXIP retroviral vector and the packaging vector were co-transfected into HEK293T (RRID: CVCL_0063) cells using Lipofectamine 3000 (Invitrogen, Waltham, MA, USA, #L3000015). After 48 h, the viral supernatant was collected, concentrated by adding a viral concentration solution, and incubated overnight. The viral solution was then centrifuged, and the concentrated viral solution was used to infect target cells in the presence of 4 μg/mL polybrene (Nacalai Tesque, #12,996–81). Stable cell lines were established by selecting infected cells with puromycin (Gibco, #A1113803). The domain-deleted NECTIN4 expression vectors were created using the IRES2-EGFP vector (RRID: Addgene_80333) (Addgene, Watertown, MA, USA, #6029–1).

Human NECTIN4-deletion using CRISPR/Cas9 technology and RNA interference

Human *NECTIN4*-knockout (KO) H322 cell lines were generated using CRISPR/Cas9 technology. Two crRNAs designed for NECTIN4 were obtained from Integrated DNA Technologies (IDT, Coralville, IA, USA). They were targeted to the sequence 5'-CCATCCACTCGTACCCCACT-3' at position 161,074,720 of the plus strand and 5'-ACTTGT GTGGTGTCCCATCC-3' at position 161,077,499 of the minus strand. Guide RNA was prepared by mixing crRNA and tracrRNA (IDT, #1,072,532), and the guide RNA were incubated for 5 min at room temperature to allow formation of the ribonucleoprotein complex (RNP complex). The RNP complex was transfected into H322 cells using RNAiMAX (Thermo Fisher Scientific, #13,778,100). The expression of NECTIN4 was evaluated by immunoblotting.

RNA interference was performed using small interfering RNA (siRNA) and Lipofectamine RNAiMAX. Cells were seeded in six-well plates, and simultaneously, a mixture of siRNA and Lipofectamine RNAiMAX was added to the wells. After 72 h, the surface expressions of NECTIN4 and CD155 were evaluated.

Immunoblot analysis

Cells were washed with ice-cold phosphate-buffered saline (PBS) and then lysed in RIPA buffer (Thermo Fisher Scientific, #89,901) containing protease and phosphatase inhibitor cocktails to prepare whole cell lysates. Cell surface proteins were isolated using the Pierce Cell Surface Biotinylation and Isolation Kit (Thermo Fisher Scientific, #A44390), following the manufacturer's instructions. All samples were fractionated by SDS–polyacrylamide gel electrophoresis on a 10% gel, and the separated proteins were transferred to a polyvinylidene difluoride membrane. The membrane was incubated overnight at 4 °C with primary antibodies. The membrane was subsequently incubated for 1 h at room temperature with horseradish peroxidase–conjugated secondary antibodies to rabbit (Cytiva, Tokyo, Japan, #NA9340) or mouse (Cytiva, #NA931VS), after which immune complexes were detected using Pierce ECL Plus Western Blotting Substrate (Thermo Fisher Scientific). Blot images were captured with the ChemiDoc Touch Imaging system (Bio-Rad, Hercules, CA, USA). Western blot quantification was performed using Image Lab 6.1 (Bio-Rad). β-Actin was used

as a loading control for total protein, and E-cadherin was used as a loading control for membrane proteins.

RT-qPCR analysis

Total RNA was extracted from cells using an RNeasy Mini Kit (Qiagen, Venlo, the Netherlands, #74,904) according to the manufacturer's instructions. cDNA was synthesized from 100 ng of total RNA using PrimeScript RT Master Mix (Takara Bio, Shiga, Japan, #RR036A). The resulting cDNA was subjected to qPCR analysis with the use of TB Green Premix Ex Taq II (Takara, #RR820A). The qPCR primers (forward and reverse, respectively) included those for 18S rRNA (5'-ACTCAACACGGGAAACCTCA-3' and 5'-AACCAGACAAATCGCTCCAC-3'), and CD155 (5'-TGATGGCTTATTACAGTGGCA-3' and 5'-GGTCGGAGATTCGTAGCTGG-3').

Flow cytometry

The surface expression of CD155 on cancer cells, and the surface or intracellular expressions of CD3, CD4, CD8, TIGIT, IFNγ, and TNFα in tumor infiltrating lymphocytes were quantified by flow cytometry. For surface staining, cells were washed with FACS buffer (PBS containing 2% FBS), and then incubated with fluorophore-conjugated antibodies diluted to the appropriate concentrations in FACS buffer at 4 °C for 1 h. After incubation, cells were washed twice with FACS buffer and analyzed. For intracellular staining, following surface staining, cells were permeabilized and incubated with antibodies diluted in permeabilization buffer at 4 °C for 1 h. Flow cytometry was performed using a FACSLyric cytometer (BD Biosciences, Franklin Lakes, NJ, USA), and data were analyzed using FlowJo software (RRID:SCR_008520) (BD Biosciences). The mean fluorescence intensity (MFI) ratio was calculated by dividing the MFI of the target antigen-specific antibody by the MFI of the isotype control antibody. To evaluate the cell surface expression of CD155 following transfection with domain-deleted NECTIN4, the IRES2-EGFP vector was used to construct each domain-deleted NECTIN4 expression vector. Transfected cells were gated based on EGFP expression, and the expression of cell surface CD155 was subsequently assessed.

Immunoprecipitation

Cells were lysed in Pierce IP Lysis Buffer (Thermo Fisher Scientific, #87,787), and the protein concentration and volume of each sample were equalized. IP antibodies were added to the lysates and incubated overnight at 4 °C with constant mixing. The antibody-protein complexes were then incubated with Pierce Protein A/G Magnetic Beads (Thermo Fisher Scientific, #88,802) for 1 h at room temperature with mixing. The bead-antibody-protein complexes were washed three times with TBS using a magnetic column, Proteins were eluted by adding Pierce IgG Elution Buffer, pH 2.0 (Thermo Fisher Scientific, #21,028) and mixing for 10 min, followed by neutralization with Neutralization Buffer (1 M Tris, pH8.5, NIPPON GENE, Tokyo, Japan, #316–90,405). The magnetic beads were removed using a magnetic stand, and the resulting protein solution was evaluated by immunoblotting.

Proximity ligation assay

Cells were fixed for 15 min with 4% paraformaldehyde in PBS, permeabilized for 10 min with 0.3% Triton X-100 in PBS, and incubated overnight at 4℃ with 1:200 dilutions of rabbit antibodies to NECTIN4 (Abcam, Cambridge, UK. #ab192033) and mouse antibodies to CD155 (BioLegend, San Diego, CA, USA. #337,602). Duolink PLA Fluorescence Kits (Sigma-Aldrich, Burlington, MA, USA. #DUO92002, 92,004, and 92,014) were used to obtain the PLA signals and images were captured by a BZ-X800 all-in-one fluorescence microscope (Keyence, Osaka, Japan).

CHX chase assay

For the cycloheximide (CHX) chase assay, cells were seeded to reach approximately 80% confluency after 48 h. Cycloheximide (Sigma-Aldrich, #239,765) was then added at a final concentration of 50 μg/mL. At the indicated time points after CHX treatment, cells were harvested, and protein lysates were analyzed by immunoblotting to assess changes in protein expression over time.

T-cell cytotoxicity assay

Peripheral blood mononuclear cells (PBMCs) were isolated from blood donated by healthy donors using BD Vacutainer Mononuclear Cell Preparation Tubes. The PBMCs were inoculated in 24-well plates (1.0×10^6 cells/well) in AIM-V medium (Thermo Fisher Scientific, #12,055,091) (1 mL/well) supplemented with 10% heat-inactivated human male AB plasma (Sigma-Aldrich, #H4522). Cells were stimulated with Dynabeads coated with anti-CD3 and anti-CD28 mAbs (Invitrogen, #DB11131) at a bead:cell ratio of 1:1. Recombinant human interleukin-2 (R&D Systems, #202-IL-010) was added at 100 IU/mL. The stimulation was carried out at 37 °C and 5% CO_2. Preactivated PBMCs were washed with PBS, resuspended in fresh medium, and directly cocultured with EBC1 cells that had been transfected with siCD155 or negative control siRNA 48 h in advance at an E:T ratio of 5:1. After 24 h of incubation, the amount of LDH in the supernatant of the coculture system was detected with the CytoTox96 nonradioactive assay

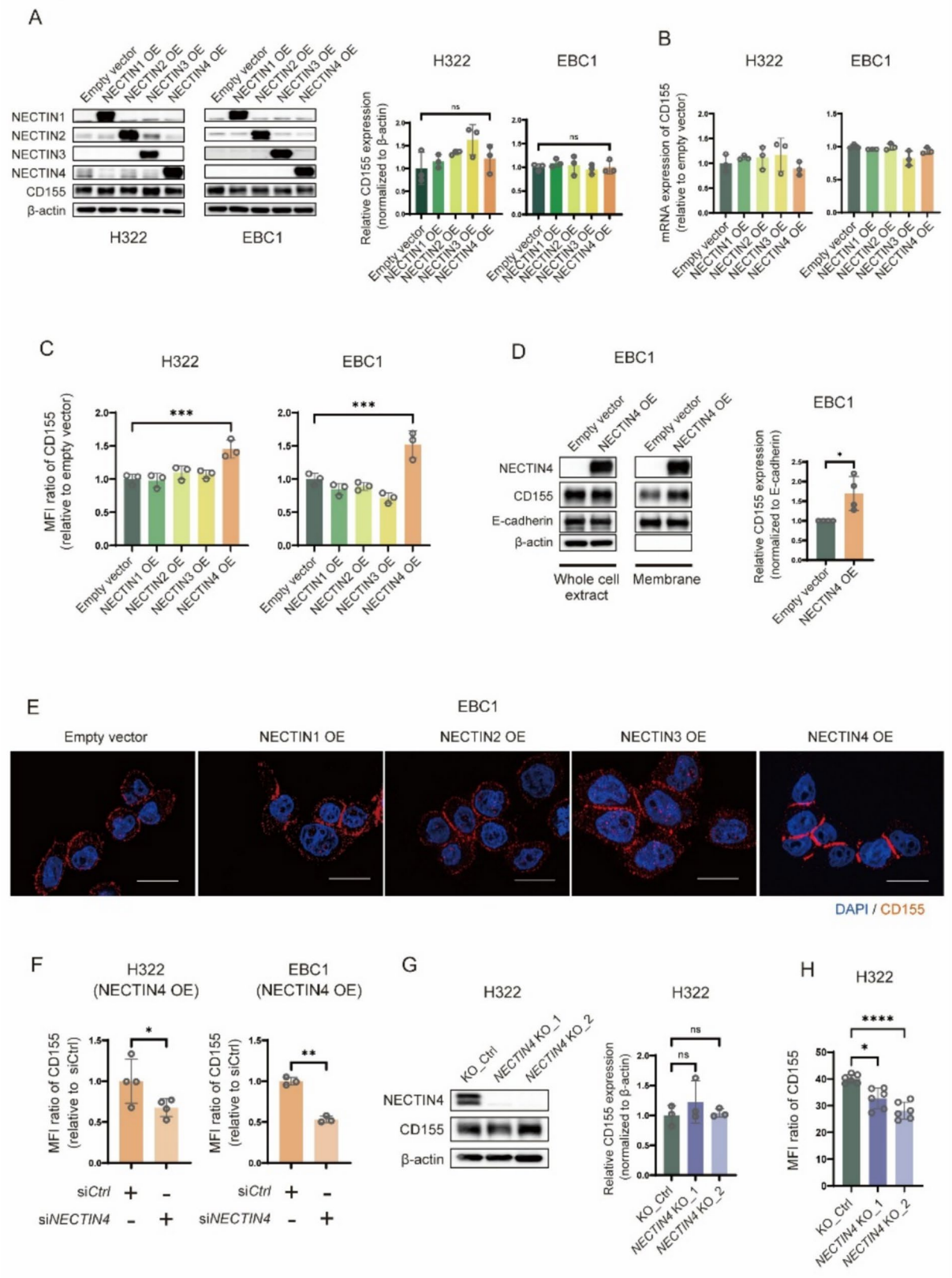
A
Empty vector
NECTIN1 OE
NECTIN2 OE
NECTIN3 OE
NECTIN4 OE
NECTIN1
NECTIN2
NECTIN3
NECTIN4
CD155
β-actin
H322
EBC1
Relative CD155 expression (normalized to β-actin)
ns
B
mRNA expression of CD155 (relative to empty vector)
C
MFI ratio of CD155 (relative to empty vector)
***
D
EBC1
E-cadherin
Whole cell extract
Membrane
Relative CD155 expression (normalized to E-cadherin)
*
E
EBC1
DAPI / CD155
F
H322 (NECTIN4 OE)
EBC1 (NECTIN4 OE)
MFI ratio of CD155 (relative to siCtrl)
*
**
siCtrl
siNECTIN4
G
KO_Ctrl
NECTIN4 KO_1
NECTIN4 KO_2
Relative CD155 expression (normalized to β-actin)
H
****

◂**Fig. 1** Cell surface expression of CD155 in NECTIN-overexpressing or -depleted NSCLC cells. **A**, Immunoblot analysis of total CD155 abundance in cell lysates in NECTIN1, 2, 3, or 4-overexpressing H322 and EBC1 cells. **B**, mRNA level of CD155 in NECTIN-overexpressing H322 and EBC1 cells by RT-qPCR. The relative quantification was performed using the ΔCt method with 18S rRNA as an internal control. **C**, Flow cytometric analysis of CD155 at the cell surface. **D**, Whole cell lysates and cell surface protein extracts were analyzed by immunoblot analysis. **E**, Localization of CD155 was evaluated by fluorescent immunostaining in EBC1 cells overexpressing each Nectin. Nuclei were stained with 4′,6-diamidino-2-phenylindole (DAPI), and CD155 was labeled with red fluorescence. Representative images were captured using optical sectioning. Scale bars, 20 μm. **F**, NECTIN4 knockdown was performed using siRNA in NECTIN4-overexpressing H322 and EBC1 cells, and cell surface CD155 expression was evaluated by flow cytometry. **G–H**, NECTIN4 knockout was established in the H322 cell line using two different guide RNAs, and CD155 expression was assessed by immunoblotting (G) and flow cytometry (H). Experiments were performed at least in triplicate, and the data are presented as the mean ± standard deviation (SD). Western blot band intensities were quantified using Image Lab software (Bio-Rad). The relative protein expression levels were normalized to β-actin and are presented as fold changes relative to the control group. Statistical analysis was conducted using one-way ANOVA followed by Tukey's test (A, B, C), Dunnett's test (G, H), or the Student's t test (D, F). $*p<0.05$, $**p<0.01$, $***p<0.001$, $****p<0.0001$. OE, overexpression; KO, knockout

(Promega, Madison, WI, USA; #G1780) following the manufacturer's instructions. Cytotoxicity was calculated using a modified version of the standard formula: (OD[experimental] − OD[spontaneous targets] − OD[spontaneous effectors])/(OD[maximum] − OD[spontaneous targets]) × 100. This part of the present study was carried out in accordance with the Declaration of Helsinki (as revised in 2013) and was approved by the Ethics Committee of Kyushu University and Kyushu University Hospital (ethics approval ID: 22,343–00).

In vivo animal study

Female BALB/c Ajcl mice (6–8 weeks old) were purchased from CLEA Japan (Tokyo, Japan). 4T1 cells (2×10^5 cells in 100 μL of PBS) or CT26 cells (5×10^5 cells in 100 μL of PBS) were subcutaneously transplanted into the right flank of mice, and the body weight and tumor volume were monitored twice a week. One week after transplantation, tumor-bearing mice were treated intraperitoneally with monoclonal antibodies (mAbs) as follows: 200 μg of anti-PD-1 mAb (RMP1-14, BioXcell, #BE0146), 150 μg of anti-TIGIT mAb (1G9, BioXcell, #BE0274), 200 μg of control IgG2a mAb (2A3, BioXcell, #BE0089), and 150 μg of control IgG1 mAb (MOPC-21, BioXcell, #BE0083). All antibodies were administered intraperitoneally in a total volume of 100 μL of PBS. The tumor volume was calculated using the formula: length × width × width/2. Tumor measurements were performed by an observer blinded to the group assignments. Animal experiments were approved by the Kyushu University Animal Experiment Committee (approval number: A23-422–5) and were performed in accordance with Kyushu University Animal Experiment Regulations, related laws and regulations, and ARRIVE (Animal Research: Reporting of In Vivo Experiments) guidelines.

Statistical analysis

Statistical analyses were performed using GraphPad Prism software (RRID: SCR_002798). All in vitro experiments were conducted at least three times, while in vivo experiments were performed at least twice. For comparisons involving more than two groups, one-way ANOVA was used, followed by Tukey's multiple comparison test or Dunnett's test, as appropriate. For comparisons between two groups, the Student's t-test was used. Data are presented as the mean ± standard deviation (SD). A p-value less than 0.05 was considered statistically significant.

Data availability

All data generated or analyzed during this study are included in this published article and its supplementary information files. The raw data analyzed during the current study are available from the corresponding author upon reasonable request.

Results

NECTIN4 is involved in the regulation of the cell surface expression of CD155 in NSCLC cells

To explore the potential regulation of CD155 expression by Nectin family members in NSCLC cells, we stably overexpressed each Nectin (NECTIN1, 2, 3, and 4) in H322 and EBC1 cells (Fig. 1A). The overexpression of NECTIN1, NECTIN2, NECTIN3, or NECTIN4 did not alter the total abundance of CD155 protein in cell lysates (Fig. 1A), or the abundance of CD155 mRNA (Fig. 1B). However, the overexpression of NECTIN4 significantly increased the cell surface expression of CD155 compared with control cells as determined by flow cytometry (Fig. 1C, Supplementary Fig. S1A). To evaluate whether this change was also observed in other NSCLC cell lines, we generated NECTIN4-overexpressing A549, H1437, and H2009 cell lines. The cell surface expression of CD155 in all of these cell lines was significantly increased compared with control cells (Supplementary Fig. S1B), without changing the total protein level or mRNA expression of CD155 (Supplementary Fig. S1C, S1D). To validate these results, cell membrane proteins were collected by biotin labeling, and the expression of cell surface CD155 in EBC1 cells was assessed by

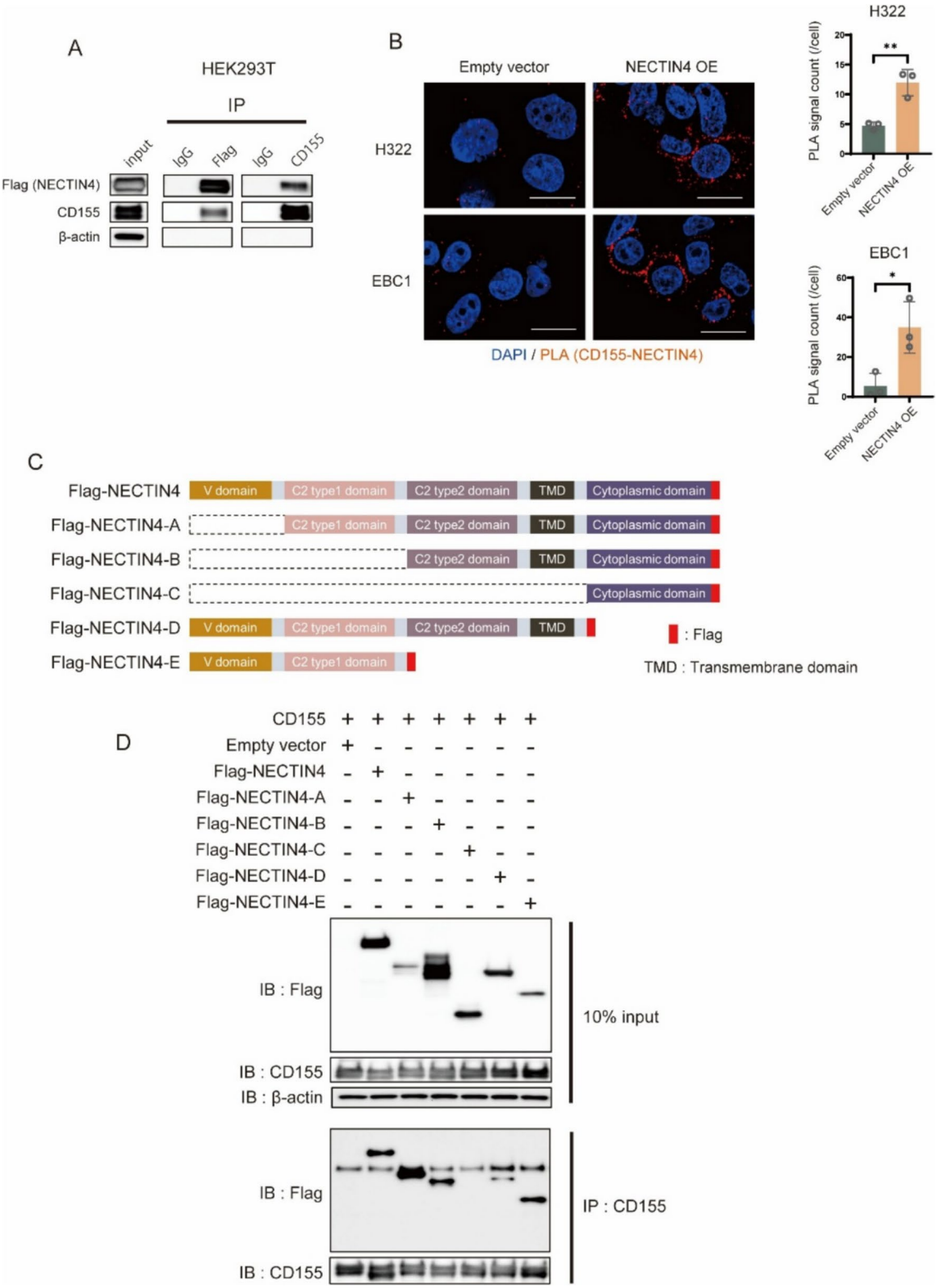

immunoblot analysis. Consistent with the flow cytometry results, CD155 expression in the cell membrane compartment was increased in NECTIN4-overexpressing cells compared with control cells (Fig. 1D). Furthermore, using fluorescent immunostaining, we evaluated the localization of CD155 in EBC1 cells overexpressing each Nectin and found that CD155 was markedly clustered on the cell surface in NECTIN4-overexpressing cells, which was not seen with

◂**Fig. 2** Evaluation of NECTIN4 and CD155 interactions and colocalization. **A**, Co-immunoprecipitation (Co-IP) experiments were performed using HEK293T cells transfected with CD155 and Flag-NECTIN4 expression vectors. Cell lysates were immunoprecipitated using Flag antibody or CD155 antibody, and immunoblotting was performed. Mouse IgG was used as a control for immunoprecipitation. **B**, A proximity ligation assay (PLA) targeting CD155 and NECTIN4 was performed in empty vector control and NECTIN4 overexpressing H322 and EBC1 cell lines. The close colocalization of CD155 and NECTIN4 was detected by red fluorescent signals. Nuclei were stained with DAPI. Scale bars, 20 µm. The number of PLA signals indicating colocalization of CD155 and NECTIN4 was determined from z-projection images generated by z-stacking of optical sections for individual cells. **C**, Schematic diagram of domain-deleted Flag-NECTIN4. **D**, HEK293T cells were co-transfected with the CD155 expression vector and full-length Flag-NECTIN4 or domain-deleted Flag-NECTIN4 expression vectors, followed by co-immunoprecipitation. As references, input samples were analyzed by immunoblotting, and samples immunoprecipitated with CD155 antibody were detected with Flag antibody by immunoblotting. Statistical analysis was conducted using Student's t test. *$p < 0.05$, **$p < 0.01$. OE, overexpression

other Nectins (Fig. 1E). To assess whether the upregulation of cell membrane CD155 in NECTIN4-overexpressing cells was an effect of NECTIN4, we evaluated the cell surface expression of CD155 in NECTIN4-overexpressing H322 and EBC1 cells after the knockdown of NECTIN4 using siRNA. The knockdown of NECTIN4 led to a significant decrease in the cell surface expression of CD155 in NECTIN4-overexpressing H322 and EBC1 cells (Fig. 1F, Supplementary Fig. S1E). Furthermore, the knockdown of endogenous NECTIN4 in H322 and H2009 cells, which have relatively high endogenous NECTIN4 expression (Supplementary Fig. S1F), led to a significant decrease in the cell surface expression of CD155 (Supplementary Fig. S1G). NECTIN4-knockout using two different gRNAs also led to a significant reduction in cell surface CD155 in H322 cells without changing the total protein level or mRNA expression of CD155 (Fig. 1G, 1H, Supplementary Fig. S1H). By contrast, it was found that overexpression of CD155 did not increase the cell surface expression of NECTIN4 (Supplementary Fig. S1I and S1J). Taken together, these data indicate that NECTIN4 positively regulates the cell surface expression of CD155 in NSCLC cells.

NECTIN4 and CD155 co-localize and interact with each other through their extracellular domains

To investigate whether NECTIN4 and CD155 interacted with each other, the expression vectors of FLAG-NECTIN4 and CD155 were co-transfected into HEK293T cells. Immunoprecipitation analysis revealed an interaction between NECTIN4 and CD155 by the ectopic overexpression of these proteins (Fig. 2A). To evaluate the interaction and plasma membrane localization of the two proteins further, PLA was performed to confirm their proximity and protein localization in H322 and EBC1 cells. Few PLA fluorescence signals were observed in control cells, whereas many fluorescence signals were detected in NECTIN4-overexpressing cells, predominantly on the cell surface (Fig. 2B). In contrast, when evaluating the colocalization of each Nectin with CD155 using PLA in EBC1 cells overexpressing NECTIN1, 2, or 3, the colocalization was not as evident as in NECTIN4-overexpressing cells (Supplementary Fig. S2A, S2B). The Nectin family belongs to the immunoglobulin superfamily and its members have three immunoglobulin-like domains (one IgV domain and two IgC domains) in the ectodomain as well as a transmembrane domain and cytoplasmic domain (20, 21). To determine which domain of NECTIN4 interacted with CD155, we constructed expression vectors for FLAG-NECTIN4 with specific domain deletions (Fig. 2C) and transfected HEK293T cells with these individual vectors and CD155 vectors. Immunoprecipitation revealed that the C2 type 2 domain binds to CD155, and that either or both of the V domain and C2 type 1 domain can also interact with CD155 (Fig. 2D).

V domain and C2 type1 domains of NECTIN4 have critical roles in the NECTIN4-mediated upregulation of cell surface CD155 expression

To investigate the critical domain of NECTIN4 involved in the upregulation of CD155 cell surface expression, we constructed various expression vectors with deletions in each domain (Fig. 3A) and evaluated the change in the expression level of cell surface CD155 by flow cytometry in EBC1 cells transfected with these constructs (Supplementary Fig. S3A). Although the constructs of full-length NECTIN4, or NECTIN4 lacking the C2 type2 domain (del_C2-2) or the cytoplasmic domain (del_cyto) showed a significant increase in cell surface CD155 expression, those of NECTIN4 lacking the V domain (del_V) or the C2 type1 domain (del_C2-1) did not show such an increase (Fig. 3B). These results indicate that the V domain and C2 type1 domain have critical roles in the NECTIN4-mediated upregulation of cell surface CD155 expression. On the basis of these results, it was suggested that NECTIN4 binds to CD155 via its extracellular domain, thereby stabilizing CD155 on the cell surface and contributing to its increased expression there. To further investigate this, we performed a cycloheximide (CHX) chase assay to evaluate the time-dependent reduction of CD155 on NECTIN4-overexpressing and control cells. The results showed that CD155 degradation was slower in NECTIN4-overexpressing cells after CHX treatment, and the expression level of CD155 at 24 h after treatment tended to be higher in NECTIN4-overexpressing cells than in the control (Supplementary Fig. S3B and S3C).

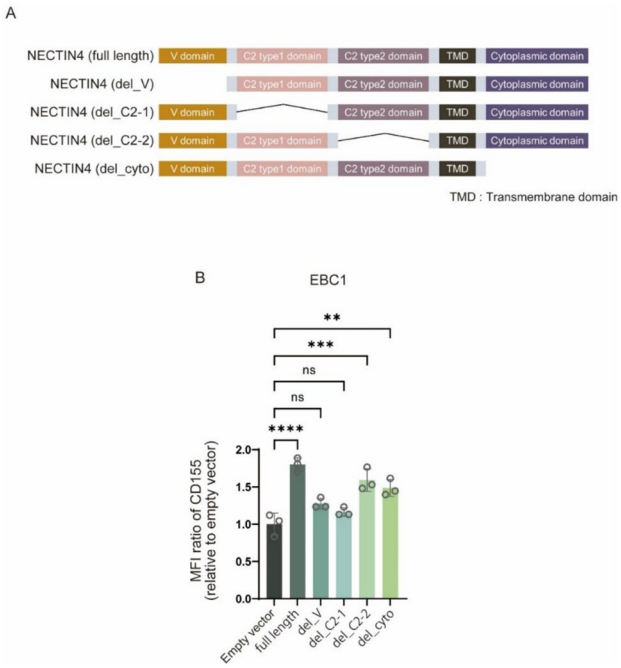

Fig. 3 Identification of NECTIN4 domains involved in the cell surface expression of CD155. **A**, Schematic diagram of domain-deleted NECTIN4. **B**, Full-length NECTIN4 or NECTIN4 with deletions in each domain were transfected into EBC1 cells, and cell surface CD155 expression was evaluated. Experiments were performed in triplicate, and the data are presented as the mean ± SD. Statistical analysis was conducted using one-way ANOVA followed by Tukey's test (B). $^{**}p < 0.01$, $^{***}p < 0.001$, $^{****}p < 0.0001$

Overexpression of NECTIN4 suppresses T-cell-mediated cytotoxicity, and CD155 depletion restores cytotoxic function of T cells

To assess the impact of NECTIN4-overexpressing cells on antitumor immunity, we performed a cytotoxicity assay using co-culture of tumor cells and peripheral blood mononuclear cell (PBMC)-derived T cells. NECTIN4-overexpressing EBC1 cells exhibited reduced T-cell-mediated cytotoxicity compared with control cells (Supplementary Fig. S4A). To determine whether this difference was attributable to CD155 stabilized on the cell surface by NECTIN4, we evaluated cytotoxicity following CD155 knockdown. Consistent with the findings in Supplementary Fig. S4A, NECTIN4-overexpressing cells transfected with si*Ctrl* showed significantly lower cytotoxicity than empty vector control cells (Supplementary Fig. S4B). Furthermore, knockdown of CD155 significantly enhanced cytotoxicity in both cell types, and under CD155-knockdown conditions there was no longer a difference in cytotoxicity between NECTIN4-overexpressing and EV control cells (Supplementary Fig. S4B). These results suggest that NECTIN4-overexpressing tumor cells suppress T-cell function, and that this suppression is mediated through stabilization of CD155 on the cell surface.

Overexpression of NECTIN4 in mouse cells increases the cell surface expression of CD155 and diminishes the therapeutic efficacy of anti-PD-1 antibody

The high expression of CD155 was reported to be involved in resistance to PD-1 inhibitors (12, 19, 24, 25). To investigate the impact of NECTIN4-mediated upregulation of CD155 on the efficacy of anti-PD-1 therapy, we first assessed whether NECTIN4 interacts with CD155 in mice. Co-immunoprecipitation assays using expression vectors for mouse NECTIN4 and CD155 confirmed their interaction, consistent with findings in human cells (Supplementary Fig. S5A). On the basis of these observations, we established mouse NECTIN4-overexpressing cells in 4T1, LL/2, and CT26 cells. In mouse NECTIN4-overexpressing 4T1 cells, cell surface expression of mouse CD155 was increased compared with that in control cells without changing the total protein level, recapitulating the pattern observed in human NSCLC cells (Supplementary Fig. S5B and S5C). By contrast, no increase in the cell surface expression of mouse CD155 was observed upon overexpression of mouse NECTIN4 in LL/2 and CT26 cells (Supplementary Fig. S5C). As NECTIN4 overexpression in 4T1 cells induced changes similar to those observed in human NSCLC cells, and the 4T1 model has been previously shown to be responsive to anti-PD-1 antibody (26), we evaluated the therapeutic efficacy of anti-PD-1 antibody using NECTIN4-overexpressing 4T1 cells in a syngeneic mouse model (Fig. 4A). Anti-PD-1 antibody significantly suppressed the tumor growth in control cells, but not in NECTIN4-overexpressing cells (Fig. 4B and C), suggesting that the overexpression of NECTIN4 was involved in the development of resistance to PD-1 inhibitors. Next, we considered the possibility that NECTIN4 itself might contribute to resistance to anti-PD-1 therapy, independent of changes in CD155 expression. To evaluate this, we assessed the antitumor effect of anti-PD-1 antibody using CT26 cells, in which NECTIN4 overexpression did not alter the expression of CD155 on the cell surface (Supplementary Fig. S5C). In CT26, the tumor-suppressive effect of anti-PD-1 antibody treatment was comparable between NECTIN4-overexpressing cells and control cells (Supplementary Fig. S5D, S5E). These results suggest that the resistance to anti-PD-1 therapy observed in NECTIN4-overexpressing 4T1 cells is not due to NECTIN4 itself but rather to the increased cell surface expression of CD155 induced by NECTIN4.

Next, we performed flow cytometric analysis of tumor-infiltrating lymphocytes (TILs) in NECTIN4-overexpressing 4T1 tumors, which were resistant to anti-PD-1 antibody treatment, and control 4T1 tumors, which were sensitive to

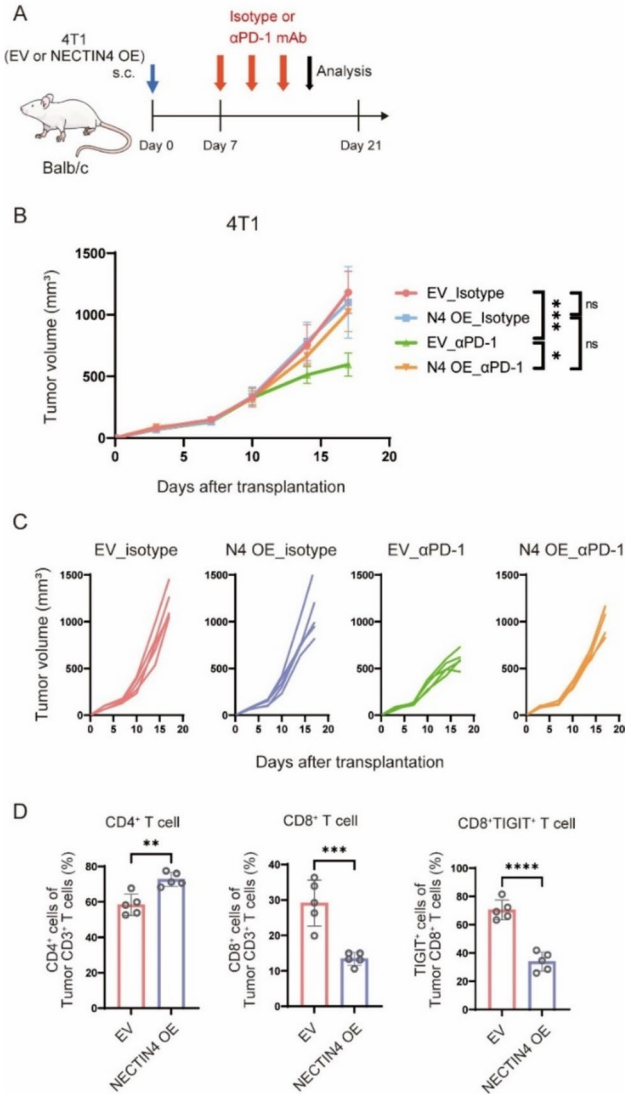

Fig. 4 Overexpression of NECTIN4 confers resistance to PD-1 inhibitors. **A**, Schematic representation of the experiment: the subcutaneous transplantation of 4T1 EV control or NECTIN4-overexpressing cells, followed by treatment with anti-PD-1 antibody. The treatment was initiated on day 7 after tumor transplantation and administered every three days for a total of three times. Anti-PD-1 mAb, or IgG2a isotype were administered at a dose of 200 μg. **B**, Graph showing tumor volumes after transplantation. Tumor volumes were calculated using the formula: length × width × width/2. **C**, Individual tumor volume progression in each group. **D**, Analysis of tumor-infiltrating lymphocytes (TILs) by flow cytometry. Experiments were conducted with five mice per group and the data are presented as the mean ± SD. All in vivo experiments were performed in duplicates, with similar results. Statistical analysis was conducted using one-way ANOVA followed by Tukey's test (B) or Student's t-test (D). $*p < 0.05$, $**p < 0.01$, $***p < 0.001$, $****p < 0.0001$. EV, empty vector; OE, overexpression

it. We found that the proportion of $CD8^+$ T cells among $CD3^+$ T cells was significantly reduced in the tumor microenvironment of NECTIN4-overexpressing tumors compared with control tumors under anti-PD-1 antibody treatment. (Fig. 4D, Supplementary Fig. S6A, S6B). In particular, a significant decrease in the proportion of $TIGIT^+$ $CD8^+$ cells was observed in NECTIN4-overexpressing cells compared with control cells under treatment with anti-PD-1 antibody treatment (Fig. 4D). To evaluate the effector function of tumor-infiltrating $CD8^+$ T cells, we assessed the proportion of IFNγ- and TNFα- positive $CD8^+$ T cells and found no difference between control cells and NECTIN4-overexpressing cells (Supplementary Fig. S6B). These findings suggest that the decrease in the number of $TIGIT^+$ $CD8^+$ T cells in the tumor microenvironment was associated with the resistance to anti-PD-1 antibody in NECTIN4-overexpressing 4T1 cells.

Anti-TIGIT antibody restores the sensitivity of NECTIN4-overexpressing cells to anti-PD-1 antibody

Next, to evaluate whether the low efficacy of anti-PD-1 antibody for mouse NECTIN4-overexpressing 4T1 cells was related to the difference in CD155 expression, we evaluated the additional effect of anti-TIGIT antibody, which suppressed the CD155/TIGIT axis (Fig. 5A). In control cells, tumor growth was effectively suppressed by anti-PD-1 antibody monotherapy without the additional effect of anti-TIGIT antibody (Fig. 5B, C and D). In NECTIN4-overexpressing 4T1 cells, although anti-PD-1 antibody monotherapy did not show a marked inhibition of tumor growth, combination therapy with anti-PD-1 and anti-TIGIT antibodies significantly suppressed tumor growth (Fig. 5B, C and D). No apparent reduction in the proportion of $CD8^+$ T cells or $TIGIT^+$ $CD8^+$ cells was observed in NECTIN4-overexpressing cells under the combination therapy (Fig. 5E). However, there was a tendency for a high proportion of IFNγ-positive cells among tumor-infiltrating $CD8^+$ T cells (Supplementary Fig. S6C). These results suggest that combination treatment with anti-TIGIT antibody and anti-PD-1 antibody prevented the reduction of $TIGIT^+$ $CD8^+$ cells and promoted the infiltration of $IFN\gamma^+$ $CD8^+$ T cells in NECTIN4-overexpressing tumors.

Discussion

In this study, we demonstrated that NECTIN4 upregulated the cell surface expression of CD155, and contributed to resistance to PD-1 inhibitors. We revealed that NECTIN4 overexpression led to an increase in the cell surface expression of CD155 without affecting transcriptional levels of CD155 in NSCLCs. We also found that this change was related to a direct interaction between NECTIN4 and CD155, resulting in the stabilization of CD155 on the cell

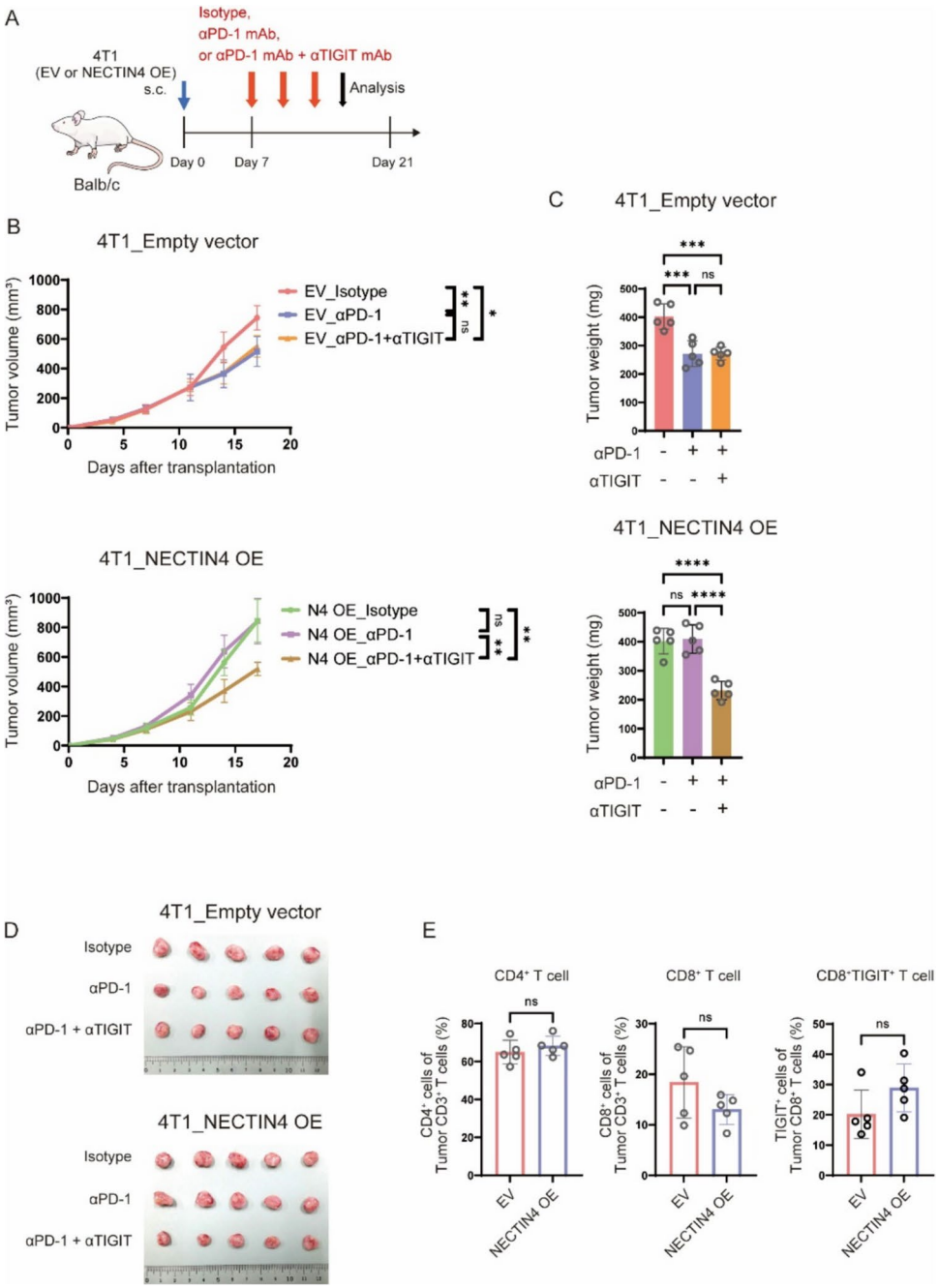

Fig. 5 Overcoming anti-PD-1 antibody resistance in NECTIN4-overexpressing 4T1 cells by combination therapy with anti-TIGIT antibody. **A**, Schematic representation of the experiment: the subcutaneous transplantation of 4T1 EV control or NECTIN4-overexpressing cells, followed by treatment with anti-PD-1 antibody alone or in combination with anti-TIGIT antibody. The treatment was initiated on day 7 after tumor transplantation and administered every three days for a total of three times. Anti-PD-1 mAb, or IgG2a isotype were administered at a dose of 200 μg, and anti-TIGIT mAb or IgG1 isotype were administered at a dose of 150 μg. **B**, Graph showing tumor volume progression after transplantation. **C**, Comparison of tumor weights in each group, measured post-excision. **D**, Photographs of tumors excised two days after the completion of treatment. **E**, Analysis of tumor-infiltrating lymphocytes (TILs) by flow cytometry. Experiments were conducted with five mice per group and the data are presented as the mean ± SD. All in vivo experiments were performed in duplicates, with similar results. Statistical analysis was conducted using one-way ANOVA followed by Tukey's test (B, C) or Student's t-test (E). *$p < 0.05$, **$p < 0.01$, ***$p < 0.001$, ****$p < 0.0001$. EV, empty vector; OE, overexpression

surface. In syngeneic mouse cancer models, increased cell surface CD155 associated with the overexpression of NECTIN4 promoted resistance to anti-PD-1 antibody treatment and sensitivity to combined anti-PD-1 and anti-TIGIT antibody treatment.

Several studies have reported on the regulatory mechanisms of CD155 expression (27–32). However, the mechanisms of the post-translational regulation of CD155 are poorly understood. Here, we found that NECTIN4 positively regulated CD155 cell surface expression in NSCLC cells. Although the interaction between NECTIN4 and CD155 has not been previously reported, our co-immunoprecipitation experiments showed that these two exogenously introduced molecules interacted directly. As shown in Fig. 2A, two bands of CD155 were observed in the input and IP-CD155 samples, whereas only a single band corresponding to a lower molecular weight was detected in the IP-FLAG sample. Because glycosylation of CD155 can alter its binding affinity to receptors (33), post-translational modifications such as glycosylation may influence the interaction between NECTIN4 and CD155. The PLA assay also indicated the proximity of NECTIN4 and CD155 on the cell surface,

although these results were not observed with other Nectins. Taken together with the decreased cell surface expression of CD155 observed after knockout or knockdown of endogenous NECTIN4, it is plausible that endogenous NECTIN4 contributes to the stabilization of CD155 on the cell surface. Our results have thus revealed a previously unrecognized mechanism related to the post-translational regulation of CD155 expression in NSCLC.

Although members of the Nectin family share similar structural features, it remains unclear why NECTIN4 contributes to the stabilization of CD155 in humans. A previous study showed that NECTIN1 and NECTIN2 tend to form stronger homodimers compared with NECTIN3 and NECTIN4 (34). Therefore, NECTIN3 and NECTIN4 may have a greater propensity to interact with other molecules, potentially contributing to the regulation of CD155. Although the exact mechanism by which NECTIN4 stabilizes CD155 on the cell surface remains unclear, our CHX chase assay showed that CD155 degradation was delayed in NECTIN4-overexpressing cells (Supplementary Fig. S3B and S3C). This suggests that NECTIN4 may retain CD155 on the cell surface and thereby inhibit its subsequent internalization and degradation. Fluorescent immunostaining data shown in Fig. 1E revealed that the stabilization of CD155 on the cell surface due to NECTIN4 overexpression was particularly pronounced at cell–cell contact sites. Because CD155 has been reported to undergo internalization through interaction with NECTIN3 at cell–cell contact sites (22, 23), our results suggest that NECTIN4 may stabilize CD155 on the cell surface by inhibiting its internalization at these junctions. Further studies are needed to clarify this mechanism.

CD155, a ligand for TIGIT, was reported to suppress the cytotoxic activity of T cells and contribute to resistance to PD-1 inhibitory therapy (12). In our study, the overexpression of NECTIN4 increased the surface expression of CD155 and resistance to the tumor suppressive effects of anti-PD-1 antibody in a syngeneic mouse model. When evaluating tumor-infiltrating T cells by flow cytometry, it was found that the proportion of $CD8^+$ T cells within $CD3^+$ T cells and $TIGIT^+$ T cells within $CD8^+$ T cells were reduced in NECTIN4-overexpressing tumors, although no significant differences in the effector function of $CD8^+$ T cells were observed as assessed by IFNγ and TNFα expression. Although TIGIT is known to be expressed on regulatory T cells, it is also known to be expressed on activated $CD8^+$ T cells. These results suggest that the increased tumor cell surface expression of CD155 mediated by NECTIN4 suppressed the infiltration or proliferation of $TIGIT^+CD8^+$ T cells in the tumor microenvironment via the CD155-TIGIT axis, leading to loss of the antitumor effect. This is consistent with a previous study reporting that tumor CD155 expression was negatively corelated with $CD8^+$ T cell infiltration in cervical cancer (10). We assessed the therapeutic efficacy of combining anti-PD-1 antibodies with anti-TIGIT antibodies, and significant suppression was observed in NECTIN4-overexpressing tumors. When evaluating TILs after the combination treatment with anti-PD-1 and anti-TIGIT antibodies, the decreased proportion of $CD8^+$ T cells and $CD8^+$ $TIGIT^+$ T cells in NECTIN4-overexpressing tumors treated with anti-PD-1 antibody alone was reversed. Furthermore, combination therapy tended to increase the infiltration of IFNγ + CD8 + T cells in NECTIN4-overexpressing 4T1 cells compared with controls. These results suggest that the addition of anti-TIGIT antibody to anti-PD-1 antibody relieved the suppression of $TIGIT^+CD8^+$ T cells via the CD155-TIGIT axis in NECTIN4-overexpressing tumors, leading to the restoration of antitumor effects. Our findings provide new insights into the immunomodulatory properties of NECTIN4, demonstrating that NECTIN4 not only enhances the CD155-TIGIT axis through increased CD155 cell surface expression and contributes to resistance to PD-1 inhibitory therapy, but also may serve as a predictive marker for the efficacy of the combination of anti-PD-1 and anti-TIGIT antibodies (Supplementary Fig. S7).

The TIGIT and PD-1 pathways are mechanistically interdependent, and the co-inhibition of TIGIT and PD-L1 synergistically elicited anti-tumor T-cell responses in mouse models (35, 36). Tiragolumab is a monoclonal antibody that binds to TIGIT and prevents it from binding to the high-affinity ligand CD155 (11). In the randomized phase 2 CITYSCAPE study, the combination therapy of tiragolumab plus atezolizumab, an anti-PD-L1 monoclonal antibody, demonstrated superior clinical benefit compared with atezolizumab monotherapy in terms of the objective response rate and progression-free survival in patients with PD-L1-positive NSCLC (37). Although TIGIT inhibitors appear to be promising agents for the treatment of several cancers, a valid predictor for this treatment is urgently needed. Our study demonstrated NECTIN4 stabilized CD155 on the cell surface leading to resistance to anti-PD-1 antibody monotherapy, whereas the combination therapy of anti-TIGIT and anti-PD-1 antibodies inhibited tumor growth. This suggests that NECTIN4 might be a predictor of the efficacy of PD-1 and TIGIT inhibitor therapy.

NECTIN4 itself is a promising therapeutic target in cancer because it is expressed at low levels in normal cells and is upregulated in some cancers, including NSCLC (38). Among different cancer types, NECTIN4 expression is highest in urothelial cancer, followed by breast cancer, pancreatic cancer, and NSCLC (38). Furthermore, in cancers in which NECTIN4 expression is relatively common, high NECTIN4 expression has been reported to be associated with poor prognosis (39). Enfortumab vedotin, an antibody–drug conjugate (ADC) targeting NECTIN4, has demonstrated therapeutic efficacy as a monotherapy for urothelial cancer and has been widely used in clinical practice. A combination

of enfortumab vedotin and pembrolizumab (anti-PD-1 antibody) showed superior efficacy compared with conventional platinum-based chemotherapy as a first-line treatment for urothelial cancer, marking a significant shift in treatment strategies for this disease (40). The mechanism underlying the high efficacy of this combination therapy is thought to involve the cytotoxic activity of the ADC, which increases damage-associated molecular patterns (DAMPs), thereby enhancing the therapeutic effect of anti-PD-1 antibodies (41, 42). Our study demonstrated that NECTIN4 stabilizes CD155 on the surface of tumor cells and contributes to immune evasion through the CD155–TIGIT axis. Therefore, the combination of NECTIN4-ADC and anti-PD-1 antibodies may represent a promising therapeutic strategy by not only promoting antitumor immunity through DAMP-mediated mechanisms but also by disrupting immune evasion via the CD155–TIGIT axis.

This study has several limitations. First, we did not demonstrate the association between NECTIN4 and CD155 in human clinical samples, nor the impact of the expression of NECTIN4 on the efficacy of anti-PD-1 therapy. Further research will be necessary to translate our findings into clinical applications. Second, although we evaluated how increased expression of CD155 in tumor cells affected TILs in our in vivo experiments, we did not assess its impact on other cell types. Investigating the effects of CD155 on immune cells other than T cells may further clarify how CD155 influences the tumor microenvironment. Further studies will be needed to address this issue.

In conclusion, our study demonstrated that NECTIN4 interacts with CD155 and stabilizes its cell surface expression. The increased cell surface expression of CD155 regulated by NECTIN4 leads to resistance to PD-1 inhibitor therapy, whereas the combination therapy of anti-PD-1 antibody and anti-TIGIT antibody significantly suppressed tumor growth. Our findings suggest that the NECTIN4/CD155 interaction has an important role in anti-tumor immunity in NSCLC and that treatment with drugs targeting the CD155-TIGIT axis or NECTIN4, in combination with PD-1/PD-L1 inhibitor, is a promising strategy for cancers with high NECTIN4 expression.

Supplementary Information The online version contains supplementary material available at https://doi.org/10.1007/s00262-025-04079-z.

Acknowledgements The Research Support Center, Research Center for Human Disease Modeling, Kyushu University Graduate School of Medical Sciences, for technical assistance

Authors' contributions S. M: Methodology, formal analysis, data curation, investigation, writing–original draft. Y. Y: Conceptualization, methodology, formal analysis, data curation, investigation, funding acquisition, project administration, writing–original draft, writing–review and editing. E. I: Methodology, writing–review and editing. T. N: Methodology, writing–review and editing. R. I: Methodology, writing–review and editing. D. S: Methodology, writing–review and editing. K. O: Methodology, writing–review and editing. K. T: Methodology, writing–review and editing. I. O: Supervision, writing–review and editing.

Data availability No datasets were generated or analysed during the current study.

Declarations

Conflict of interest Y.Y. has received honoraria from Ono Pharmaceutical, Takeda Pharmaceutical. E.I. has received honoraria from Chugai Pharmaceutical and AstraZeneca. K.T. has received honoraria from Chugai Pharmaceutical, AstraZeneca, Ono Pharmaceutical, Bristol-Myers Squibb, Eli Lilly, Takeda Pharmaceutical, Daiichi-Sankyo, and MSD. I.O. has received honoraria and research funding from Chugai Pharmaceutical, AstraZeneca, Ono Pharmaceutical, Taiho Pharmaceutical, MSD, Eli Lilly, Boehringer Ingelheim, and Bristol-Myers Squibb as well as honoraria from Pfizer and research funding from Astellas, Novartis, Takeda Pharmaceutical, Daiichi Sankyo, Haihe Biopharma, and AbbVie. The remaining authors declare no financial or non-financial competing interests.

Ethical approval Animal studies: Animal experiments were approved by the Kyushu University Animal Experiment Committee (approval number: A23-422–4) and were performed in accordance with Kyushu University Animal Experiment Regulations, related laws and regulations, and ARRIVE (Animal Research: Reporting of In Vivo Experiments) guidelines. Approval of the research protocol by an institutional review board: The study was approved by the Ethics Committee of Kyushu University and Kyushu University Hospital (ethics approval ID: 2021–289, 22,343–00).

Informed consent Informed consent was obtained from all healthy donors.

References

1. Reck M, Rodriguez-Abreu D, Robinson AG, Hui R, Csoszi T, Fulop A et al (2016) Pembrolizumab versus chemotherapy for PD-L1-positive non-small-cell lung cancer. N Engl J Med 375:1823–1833
2. Gandhi L, Rodriguez-Abreu D, Gadgeel S, Esteban E, Felip E, De Angelis F et al (2018) Pembrolizumab plus chemotherapy in metastatic non-small-cell lung cancer. N Engl J Med 378:2078–2092
3. Paz-Ares L, Luft A, Vicente D, Tafreshi A, Gumus M, Mazieres J et al (2018) Pembrolizumab plus chemotherapy for squamous non-small-cell lung cancer. N Engl J Med 379:2040–2051

4. Herbst RS, Giaccone G, de Marinis F, Reinmuth N, Vergnenegre A, Barrios CH et al (2020) Atezolizumab for first-line treatment of PD-L1-selected patients with NSCLC. N Engl J Med 383:1328–1339
5. Rizvi NA, Hellmann MD, Snyder A, Kvistborg P, Makarov V, Havel JJ et al (2015) Cancer immunology. Mutational landscape determines sensitivity to PD-1 blockade in non-small cell lung cancer. Science 348:124–128
6. Yi M, Jiao D, Qin S, Chu Q, Wu K, Li A (2019) Synergistic effect of immune checkpoint blockade and anti-angiogenesis in cancer treatment. Mol Cancer 18:60
7. Qin S, Xu L, Yi M, Yu S, Wu K, Luo S (2019) Novel immune checkpoint targets: moving beyond PD-1 and CTLA-4. Mol Cancer 18:155
8. Bai X, Yi M, Jiao Y, Chu Q, Wu K (2019) Blocking TGF-beta signaling to enhance the efficacy of immune checkpoint inhibitor. Onco Targets Ther 12:9527–9538
9. Weber R, Fleming V, Hu X, Nagibin V, Groth C, Altevogt P et al (2018) Myeloid-derived suppressor cells hinder the anti-cancer activity of immune checkpoint inhibitors. Front Immunol 9:1310
10. Liu L, Wang A, Liu X, Han S, Sun Y, Zhang J et al (2022) Blocking TIGIT/CD155 signalling reverses CD8(+) T cell exhaustion and enhances the antitumor activity in cervical cancer. J Transl Med 20:280
11. Chiang EY, Mellman I (2022) TIGIT-CD226-PVR axis: advancing immune checkpoint blockade for cancer immunotherapy. J Immunother Cancer 10:e004711
12. Kawashima S, Inozume T, Kawazu M, Ueno T, Nagasaki J, Tanji E et al (2021) TIGIT/CD155 axis mediates resistance to immunotherapy in patients with melanoma with the inflamed tumor microenvironment. J ImmunoTherapy Cancer 9(11):e003134. https://doi.org/10.1136/jitc-2021-003134
13. Zhan M, Zhang Z, Zhao X, Zhang Y, Liu T, Lu L et al (2022) CD155 in tumor progression and targeted therapy. Cancer Lett 545:215830
14. Molfetta R, Zitti B, Lecce M, Milito ND, Stabile H, Fionda C et al (2020) CD155: a multi-functional molecule in tumor progression. Int J Molecular Sci 21(3):922. https://doi.org/10.3390/ijms21030922
15. Nakai R, Maniwa Y, Tanaka Y, Nishio W, Yoshimura M, Okita Y et al (2010) Overexpression of Necl-5 correlates with unfavorable prognosis in patients with lung adenocarcinoma. Cancer Sci 101:1326–1330
16. Nishiwada S, Sho M, Yasuda S, Shimada K, Yamato I, Akahori T et al (2015) Clinical significance of CD155 expression in human pancreatic cancer. Anticancer Res 35:2287–2297
17. Huang DW, Huang M, Lin XS, Huang Q (2017) CD155 expression and its correlation with clinicopathologic characteristics, angiogenesis, and prognosis in human cholangiocarcinoma. Onco Targets Ther 10:3817–3825
18. Zhuo B, Li Y, Gu F, Li Z, Sun Q, Shi Y et al (2018) Overexpression of CD155 relates to metastasis and invasion in osteosarcoma. Oncol Lett 15:7312–7318
19. Lee BR, Chae S, Moon J, Kim MJ, Lee H, Ko HW, Cho BC, Shim HS, Hwang D, Kim HR, Ha S-J (2020) Combination of PD-L1 and PVR determines sensitivity to PD-1 blockade. JCI Insight. https://doi.org/10.1172/jci.insight.128633
20. Takai Y, Nakanishi H (2003) Nectin and afadin: novel organizers of intercellular junctions. J Cell Sci 116:17–27
21. Samanta D, Almo SC (2015) Nectin family of cell-adhesion molecules: structural and molecular aspects of function and specificity. Cell Mol Life Sci 72:645–658
22. Ikeda W, Kakunaga S, Itoh S, Shingai T, Takekuni K, Satoh K et al (2003) Tage4/Nectin-like molecule-5 heterophilically transinteracts with cell adhesion molecule Nectin-3 and enhances cell migration. J Biol Chem 278:28167–28172
23. Chiu DK, Yuen VW, Cheu JW, Wei LL, Ting V, Fehlings M et al (2020) Hepatocellular carcinoma cells up-regulate PVRL1, stabilizing PVR and inhibiting the cytotoxic T-Cell response via TIGIT to mediate tumor resistance to PD1 inhibitors in mice. Gastroenterology 159:609–623
24. Lepletier A, Madore J, O'Donnell JS, Johnston RL, Li XY, McDonald E et al (2020) Tumor CD155 expression is associated with resistance to anti-PD1 immunotherapy in metastatic melanoma. Clin Cancer Res 26:3671–3681
25. Jiang C, Qu X, Ma L, Yi L, Cheng X, Gao X et al (2022) CD155 expression impairs anti-PD1 therapy response in non-small cell lung cancer. Clin Exp Immunol 208:220–232
26. Kaplanov I, Carmi Y, Kornetsky R, Shemesh A, Shurin GV, Shurin MR et al (2019) Blocking IL-1beta reverses the immunosuppression in mouse breast cancer and synergizes with anti-PD-1 for tumor abrogation. Proc Natl Acad Sci U S A 116:1361–1369
27. Solecki DJ, Gromeier M, Mueller S, Bernhardt G, Wimmer E (2002) Expression of the human poliovirus receptor/CD155 gene is activated by sonic hedgehog. J Biol Chem 277:25697–25702
28. Hirota T, Irie K, Okamoto R, Ikeda W, Takai Y (2005) Transcriptional activation of the mouse Necl-5/Tage4/PVR/CD155 gene by fibroblast growth factor or oncogenic Ras through the Raf-MEK-ERK-AP-1 pathway. Oncogene 24:2229–2235
29. Kamran N, Takai Y, Miyoshi J, Biswas SK, Wong JSB, Gasser S (2013) Toll-like receptor ligands induce expression of the costimulatory molecule CD155 on antigen-presenting cells. PLoS ONE 8(1):e54406. https://doi.org/10.1371/journal.pone.0054406
30. Soriani A, Fionda C, Ricci B, Iannitto ML, Cippitelli M, Santoni A (2013) Chemotherapy-elicited upregulation of NKG2D and DNAM-1 ligands as a therapeutic target in multiple myeloma. Oncoimmunology 2:e26663
31. Fionda C, Abruzzese MP, Zingoni A, Soriani A, Ricci B, Molfetta R et al (2015) Nitric oxide donors increase PVR/CD155 DNAM-1 ligand expression in multiple myeloma cells: role of DNA damage response activation. BMC Cancer 15:17
32. Gao J, Zheng Q, Shao Y, Wang W, Zhao C (2018) CD155 downregulation synergizes with adriamycin to induce breast cancer cell apoptosis. Apoptosis 23:512–520
33. Tahara S, Okumura G, Matsuo T, Shibuya A, Shibuya K (2024) Essential role of CD155 glycosylation in functional binding to DNAM-1 on natural killer cells. Int Immunol 36:317–325
34. Harrison OJ, Vendome J, Brasch J, Jin X, Hong S, Katsamba PS et al (2012) Nectin ectodomain structures reveal a canonical adhesive interface. Nat Struct Mol Biol 19:906–915
35. Johnston RJ, Comps-Agrar L, Hackney J, Yu X, Huseni M, Yang Y et al (2014) The immunoreceptor TIGIT regulates antitumor and antiviral CD8(+) T cell effector function. Cancer Cell 26:923–937
36. Banta KL, Xu X, Chitre AS, Au-Yeung A, Takahashi C, O'Gorman WE et al (2022) Mechanistic convergence of the TIGIT and PD-1 inhibitory pathways necessitates co-blockade to optimize anti-tumor CD8(+) T cell responses. Immunity 55(512–26):e9
37. Cho BC, Abreu DR, Hussein M, Cobo M, Patel AJ, Secen N et al (2022) Tiragolumab plus atezolizumab versus placebo plus atezolizumab as a first-line treatment for PD-L1-selected non-small-cell lung cancer (CITYSCAPE): primary and follow-up analyses of a randomised, double-blind, phase 2 study. Lancet Oncol 23:781–792
38. Challita-Eid PM, Satpayev D, Yang P, An Z, Morrison K, Shostak Y et al (2016) Enfortumab vedotin antibody-drug conjugate targeting nectin-4 is a highly potent therapeutic agent in multiple preclinical cancer models. Cancer Res 76:3003–3013
39. Chatterjee S, Sinha S, Kundu CN (2021) Nectin cell adhesion molecule-4 (NECTIN-4): a potential target for cancer therapy. Eur J Pharmacol 911:174516

40. Powles T, Valderrama BP, Gupta S, Bedke J, Kikuchi E, Hoffman-Censits J et al (2024) Enfortumab vedotin and pembrolizumab in untreated advanced urothelial cancer. N Engl J Med 390:875–888
41. Hoimes CJ, Flaig TW, Milowsky MI, Friedlander TW, Bilen MA, Gupta S et al (2023) Enfortumab vedotin plus pembrolizumab in previously untreated advanced urothelial cancer. J Clin Oncol 41:22–31
42. Krysko DV, Garg AD, Kaczmarek A, Krysko O, Agostinis P, Vandenabeele P (2012) Immunogenic cell death and DAMPs in cancer therapy. Nat Rev Cancer 12:860–875